

# 428. Development of micro ultrasonic motor for surgery

**Shigeki Toyama and Tomoaki Mashimo**

Tokyo University of Agriculture and Technology, Tokyo, Japan

*(Received 11 January 2007; accepted 10 March 2007)*

**Abstract.** We present a micro ultrasonic motor having rotary and linear motions for endovascular diagnosis and surgery. The stator prototype is a cube of side 3.5mm, and the main body is fabricated as a single metallic cube with a through-hole at the center. Four piezoelectric elements are bonded to the sides of the stator. When AC voltage is applied to the piezoelectric elements, the circumference of the stator generates elliptical motions. We can obtain the output from a shaft inserted through the hole. We developed the first prototype of the stator, and determined the rotary-linear motion.

**Keywords:** piezoelectric actuator, endovascular medicine, micro mechanism, rotary-linear, ultrasonic motor

## Introduction

Endovascular surgery is a method of minimally invasive surgery that is capable of accessing many regions of the body via blood vessels. Most endovascular techniques involve the percutaneous insertion of a catheter through the skin into a large blood vessel. Typically, the chosen blood vessel is the femoral artery or vein. The catheter is injected with a radio-opaque contrast medium visible on live x-ray. As the contrast medium courses through the blood vessels, diagnosis images can be observed by experienced viewers. This procedure assists in the diagnosis of diseases such as thrombosis.

Recently several rotational surgery devices, called atherectomy and interventional ultrasound (IVUS), have been used for the endovascular diagnosis and surgery. The rotablator, which is one of the atherectomy has a diamond burr at the tip of catheter. After it was guided to the blockage, the diamond burr rotates at high speeds. The burr grinds the hardened plaque into small particles. Directional atherectomy was designed to remove non-calcified plaque. After insertion of the catheter, a balloon inflates, pushing the blade toward the plaque. The blade cuts away the plaque and stores it in a chamber. The balloon deflates and the plaque is removed when the catheter is withdrawn. IVUS was used for the endovascular diagnosis. IVUS is a medical imaging method with an ultrasound probe attached to the tip end of the catheter. The most valuable use of IVUS is to see the plaque, which is not visible by angiography. These devices rotate using wire by means of a driving source including a rotational motor outside the human body. In the catheters, the rotary motion is a transfer from the driving source, and the linear motion is manipulation by a human hand. In a complex and narrow blood vessels, the use of the devices is difficult because of the buckling and the inflexibility of the catheter.

We present a novel small ultrasonic motor having rotary and linear motions (rotary-linear motor). An image of its application in endovascular surgery is presented in Fig. 1. Although

there are several studies on miniature actuators [1]-[3], they only have either rotary or linear motion. The catheter using the small motor at the tip of itself generates the rotary and linear motions in the case of that the catheter is bending along blood vessel. The stator is fabricated as a rectangular metallic solid with a through-hole. The shape of the stator makes the machining easy and inexpensive. This simple structure is suitable to be miniaturized for endovascular operation. Additionally, the small rotary-linear motor has magnetic resonance imaging (MRI) compatibility. MRI, which involves a strong magnetic field, employs ultrasonic motors for moving its seat, or MRI compatible surgical robot researches. MRI can eliminate exposure to radiation from computer tomography (CT) or side effect from the contrast medium. Although diagnostic X-rays provide great benefits, their use involves some small risk of inducing cancer.

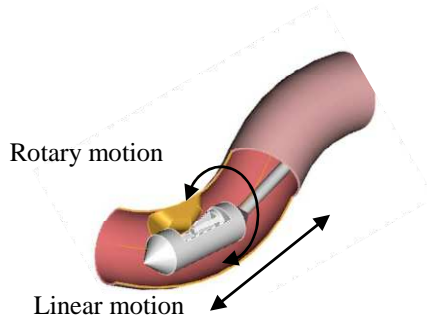


**Fig. 1.** Endovascular surgery

### Design of the rotary-linear motor

We explain the three vibration modes in the rotary-linear motor. The stator of rotary-linear motor excites distinct vibration modes in the case of rotary and linear motions. The hole of the stator generates each elliptical motion. In this paper, the "axis" is defined as the axis of the hole and is the z-axis, and the "radius" is defined as the radius of the hole of the stator. The mode of the rotary motion comprises three waves along the circumference of the through-hole ( $R_3$  mode) as illustrated in Fig. 2(a). The modes of linear motion are a first extension mode ( $T_1$  mode), as shown in Fig.2 (b), and a second extension mode ( $T_2$  mode) - in Fig. 2(c). The node of the  $T_2$  mode is median surface of the stator in perpendicular direction to the axis. The antinodes are eight corners. The two modes are excited at a single resonant frequency. Generation of the elliptical motion by the combination of the modes at a single resonant frequency has been reported by an ultrasonic linear motor and multi-degree of freedom ultrasonic motor. These involved a combination of the first extension mode and the second bending mode of a free beam or plate.

In the stator of the rotary-linear motor, the elliptical motion is generated by the  $T_1$  and  $T_2$  modes. The sequence of the displacement is given in Fig. 3(a)-(d). The  $T_1$  mode is a repeat of Fig. 3(a) and (c), and the  $T_2$  mode is a repeat of Fig. 3(b) and (d). The  $T_1$  mode has symmetry and the  $T_2$  mode has anti-symmetry with respect to the median surface. When the phase difference between  $T_1$  mode and  $T_2$  mode is  $\pi/2$ , the elliptical motion is generated. The points  $P_L$  and  $P_R$  are located at either edges of inner surface in Fig. 3(a). When the movement of the points is plotted, elliptical motion is drawn in the same direction as in Fig. 3(e) and (f). The elliptical motion therefore moves the output shaft in the direction of the axis.

Characteristic analysis using finite element method (FEM) clarifies the mode shapes and natural frequencies of the stator. The stator must be designed to have the natural frequencies such that the  $T_1$  and  $T_2$  modes accord. When the stator size is changed, the shift of the natural frequency is analyzed by FEM. The FEM model of the stator is presented in Fig. 4. The material characteristics are those of phosphor bronze. The height  $H$ , width  $W$ , and depth (length in direction to the axis)  $L$  are all 3.5 mm. The diameter of the through-hole is 2.5 mm. The number of elements in the FEM model is approximately 400. The natural frequency of  $R_3$  mode was 276 kHz. The natural frequencies of  $T_1$  mode and  $T_2$  mode are respectively 321 kHz and 322 kHz, essentially identical as expected for the cubic shape.

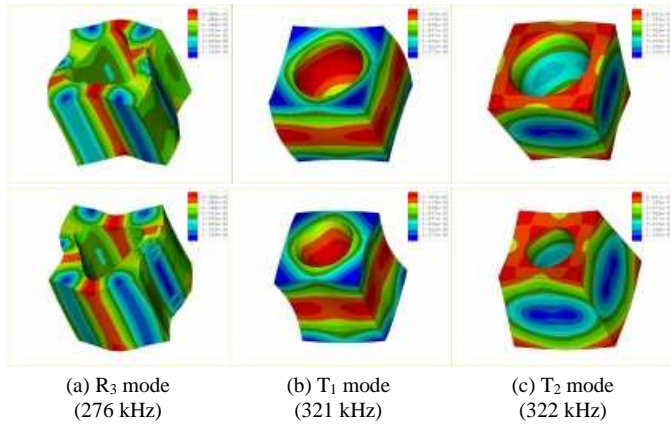


Fig. 2. Vibrational modes of the stator

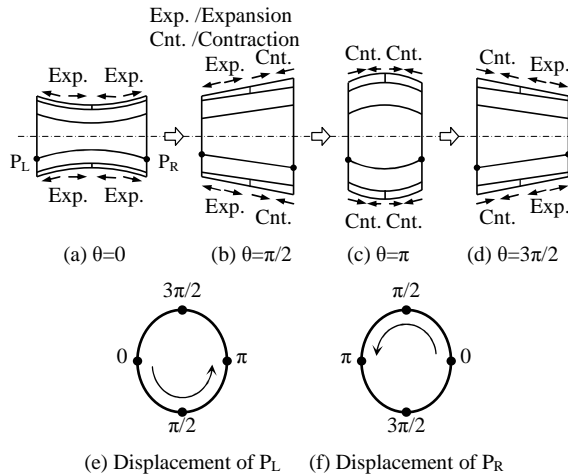
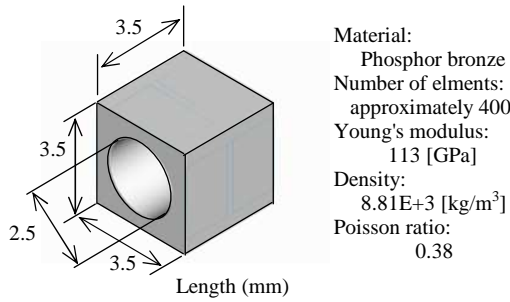


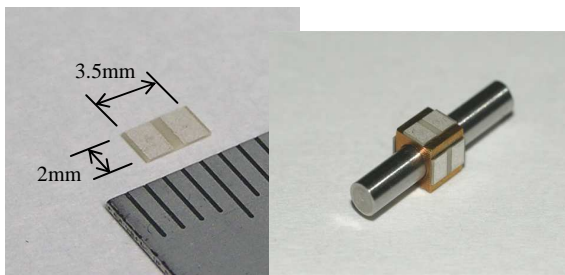
Fig. 3. Trajectory of the elliptical motions



**Fig. 4.** Model and parameters for FEM analysis

**Experimental setup**

A prototype rotary-linear motor was constructed as shown in Fig. 5. The piezoelectric element (Material C-82: Fuji Ceramics Co., Japan) is illustrated in Fig. 5 (a). It has two silver electrodes, the direction of which is polarized "positive" in one side. Another side is a silver electrode polarized "negative," this side is bonded to the side of the stator. The surface of the piezoelectric elements in contact with the stator conducts electrically to the body of the stator as well as to the ground. One of the prototypes of rotary-linear motor is presented in Fig. 5(b). Four piezoelectric elements are bonded to the sides of the stator. The measured clearance between the stator and the output shaft is approximately 10 μm. The inserted shaft can be moved by light force of hand. In the experiment, the size of the stator is a 3.5 mm cube with a hole of inner diameter 2.5 mm as in simulation (Fig. 4).



(a) Piezoelectric element (b) Prototyped rotary-linear motor

**Fig. 5.** Prototype of rotary-linear motor

The four sides of the stator are named "A" to "D" in direction to z-axis clockwise, and the positive direction of z-axis is called "p" and the negative direction is "n." Four piezoelectric elements are placed at the four sides of the stator. The amplitude of the AC voltages applied to all silver electrodes on these piezoelectric elements are given as " $E_{Ap}$ ", " $E_{An}$ " to " $E_{Dp}$ ", " $E_{Dn}$ " as shown in Fig. 6. To generate the rotation, four voltages in phase step of  $\pi/2$  are applied around the z-axis as given by:

$$E_{Ap} = E_{An} = A \sin(2\pi f_r t) \quad (1)$$

$$E_{Bp} = E_{Bn} = A \sin(2\pi f_r t + \pi/2) \quad (2)$$

$$E_{Cp} = E_{Cn} = A \sin(2\pi f_r t + \pi) \quad (3)$$

$$E_{Dp} = E_{Dn} = A \sin(2\pi f_r t + 3\pi/2) \quad (4)$$

where  $A$  is the amplitude of the applied voltages,  $f_r$  is a natural frequency exciting  $R_3$  mode. Eqs. (1)-(4) represent a traveling wave. For generating translation, the applied voltages  $E_{Ap}$ ,  $E_{An}$  to  $E_{Dp}$ ,  $E_{Dn}$  are:

$$E_{Ap} = E_{Bp} = E_{Cp} = E_{Dp} = A \sin(2\pi f_i t) \quad (5)$$

$$E_{An} = E_{Bn} = E_{Cn} = E_{Dn} = A \sin(2\pi f_i t + \pi/2) \quad (6)$$

where  $f_i$  is a natural frequency exciting  $T_1$  and  $T_2$  modes. The amplitude of the voltages  $A$  is 42  $V_{rms}$  in this experiment.

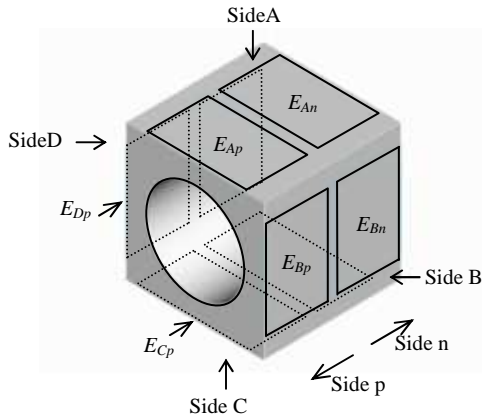


**Fig. 6.** Electrode the voltages apply

The impedance characteristics of the stator were measured by an impedance analyzer (Agilent Technologies: 4294A). The corners of the stator were fixed softly on a holder, which connects to ground. One of the cables was selected arbitrarily and was connected to the impedance analyzer. Fig. 7 presents the impedance and the frequency characteristics at 250-330 kHz. In Fig. 7, two resonances were observed at approximately 280 kHz and about 310 kHz. They are natural frequencies at which the motor generates rotary and linear motions respectively. There are two natural frequencies of  $T_1$  and  $T_2$  modes at 310 kHz redundantly. The difference between the measured resonant frequencies and the results of characteristic analysis using FEM was approximately 10 kHz or approximately 3%. This is due to the condition of the stator, such as material inhomogeneity and discrepancies in the size.

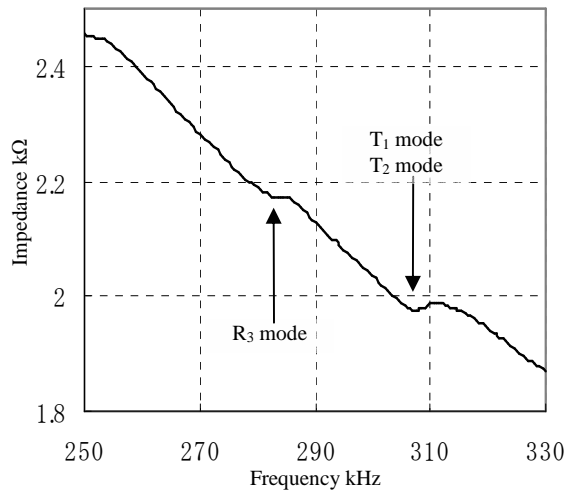


**Fig. 7.** Characteristic frequencies of the stator

### Effect from frequencies and applied voltages

The frequency and applied voltages as related to performances are essential factor for control of the rotary and linear motions and for designing improvement to performance. The characteristics of conventional micro ultrasonic motor are set out in previous studies. The performance peaks at the resonant frequency, and is movable near that frequency. Fig. 8 indicates frequency versus performance. The movable range of the rotary motion is 262-284 kHz. The peak was obtained at approximately 270 kHz. The maximum rotary speed was 260 rpm. On the other hand, the movable range of the linear motion is 300-312 kHz, the maximum linear speed was 50 mm/s at 306 kHz. Fig. 9 presents applied voltage versus performance. It is known that the performance generally increase in proportion to the applied voltages increase. The rotary-linear motor started to move at a voltage of approximately 30  $V_{rms}$  in the both directions. Both rotary and linear speeds increased in proportion to the voltage as the voltage increased. The maximum performances measured were 600 rpm and 120 mm/s at the voltage of 71  $V_{rms}$ . The torque should also increase as the voltages increases [3].

### Conclusion

In this paper we reported the development of a rotary-linear motor using a single metal stator. This rotary-linear motor was miniaturized to a smaller size than hitherto as a multi-DOF actuator. The stator was fabricated as a 3.5 millimeter cube without a special machining process. The circumference-excited  $R_3$  mode was successfully actuated to rotate the shaft. The  $T_1$  and  $T_2$  modes allowed linear motion of a linear piezoelectric actuator. In rotary motion, a performance of approximately 260 rpm and 0.1 mNm was obtained at the resonant frequency of 270 kHz, and for linear motion the performance was about 50 mm/s and 0.01 mN at 306 kHz when the applied voltages was 42  $V_{rms}$ , though the motor began to rotate at 28  $V_{rms}$ . Since the aim is to operate this rotary-linear motor in a blood vessel, it should be designed so as to rotate at lower voltages of less than 10 V.

In the future, further miniaturization and improvement of performance should be possible. In

general, ultrasonic motors employ a stator with many slits, and coating of contact surface to obtain higher performance. These should improve the outputs. On the other hand, the combination of the rotary and linear modes can generate other motion, such as helical motion. As well as other medical applications, we predict microrobotic and industrial applications. Because of the simple structure, the rotary-linear motor is likely to find many applications.

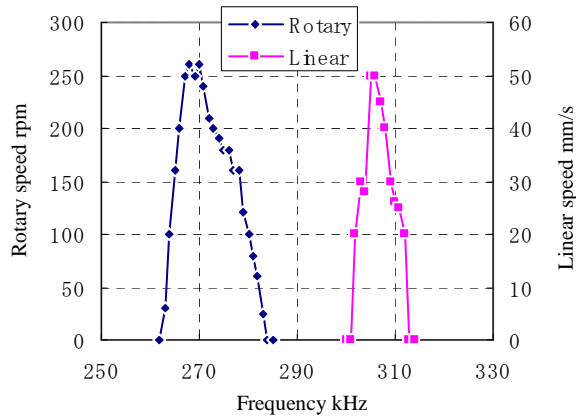


Fig. 8. Relation between frequency and performances

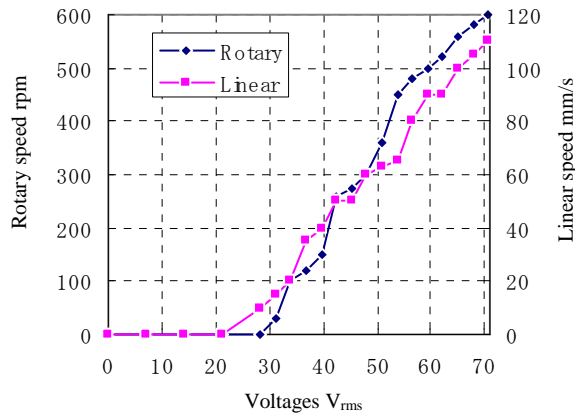


Fig. 9. Relation between voltage and performances

## References

- [1] Morita T., Kuribayashi Kurosawa M., and Higuchi T. "A cylindrical micro ultrasonic motor using PZT thin film deposited by single process hydrothermal method ( $\phi$ :2.4 mm, L=10 mm stator transducer)," IEEE Trans. Ultrasonics, Ferroelectrics and Frequency Control, vol. 45, pp. 1178-1187, 1998.
- [2] Friend J., Gouda Y., Nakamura K., and Ueha S. "A simple bidirectional linear microactuator for nanopositioning - the "Baltan" microactuator," IEEE Trans. Ultrasonics, Ferroelectrics and Frequency Control, vol. 53, pp. 1160-1168, 2006.
- [3] Kanda T., Makino A., Ono T., Suzumori K., Morita T., and Kurosawa M. K. "A micro ultrasonic motor using a micro-machined cylindrical bulk PZT transducer," Sensors and Actuators A: Physical, vol. 127, pp. 131-138, 2006.